

# Motion Analysis and Stability Control of Four-Wheeled Omnidirectional Mobile Robot under Limited Hardware Resource

**Jun-nan Li, Xiao-yu Tang\*, Fu-ren Xu and Rui-shan Huang**

School of Physics and Telecommunication Engineering South China Normal University  
Guangzhou, China

\*tangxy@scnu.edu.cn

**Abstract.** Since widely used in factories, hospitals and other workplaces, the motion stability of Mecanum omnidirectional mobile platform becomes more and more important. In this paper, an improved PID algorithm based on integral separation method, anti-integral saturation method and incomplete differential method was proposed to improve the control precision and motion stability of omnidirectional mobile robot (OMR) under limited hardware resource. From the analysis of the experimental data, it can be seen that by combining the Angle data with the motion equation, the attitude of the omnidirectional mobile platform can be adjusted in a short time, and the response speed can be greatly improved.

## 1. Introduction

With the development of modern engineering control technology and computer science, mobile robots play an important role in various fields. Among many mobile platforms, the Mecanum wheel mobile platform has gradually received more attention because of its three-degree-of-freedom mobility. Omnidirectional mobile robots (OMRS) based on Mecanum wheels are playing an increasingly important role in transportation, modern manufacturing and other fields because they realize the movement of any direction and radius in the plane [1-2].

However, Because of the special physical structure of Mecanum wheels, the movement of wheels on the ground is very susceptible to the ground friction [3], which cause OMR slide during driving and cause the actual course to deviate from the set heading frequently. In order to solve the above problems, many experts and scholars have proposed many methods to modify the attitude and position of robots. T Jilek *et al.* described kinematic models of a mobile robot with a six-wheeled chassis. At the same time, they proposed odometry method for estimation of robot's position and orientation [4]. Pouya Panahandeh *et al.* proposed two non-smooth kinematic control strategies for the posture stabilization of a differentially driven wheeled mobile robot [5]. In addition, in the field of engineering control, many excellent researchers use the method of fuzzy control to solve the sliding problem of Mecanum wheel. Zheng-cai CAO *et al.* presented a kinematic nonlinear state feedback control law to regulate the robot by the fuzzy controller [6]. Hsu-Chih Huang *et al.* presented an intelligent fuzzy motion controller for three-wheeled omnidirectional mobile robots to achieve trajectory tracking and stabilization. They used the fuzzy theory to tune the parameters of the motion controller online [7].

This paper proposes a strategy to improve the OMR course accuracy under limited hardware resource. Under the control of improved PID algorithm, the accurate control of Four-Wheeled Omnidirectional



Mobile Robot is realized by using NXP MCU, MPU9250 space motion sensor and other electronic components with reasonable price and excellent performance.

## 2. System Design of Omnidirectional Mobile Robot

The OMR in this article is composed of hardware circuit and integrated module, as shown in figure 1. Hardware circuit mainly includes power supply module, MCU main control module, angle(measurement angle of OMR) measurement circuit, motor drive circuit, etc. Integrated module includes Bluetooth module, Encoder module. Using the knowledge of electronic circuit and limited hardware resource, a complete and feasible design scheme of OMR is obtained. The control system structure is shown in figure 2.

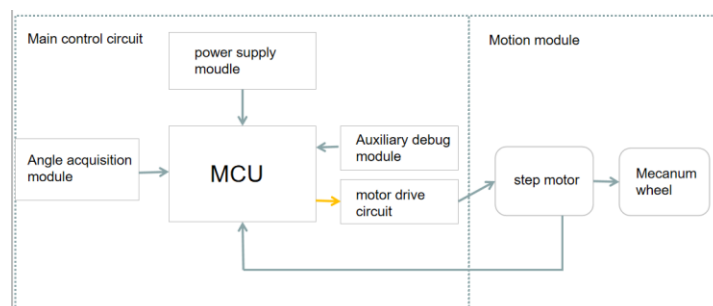


**Figure 1.** System scheme architecture diagram

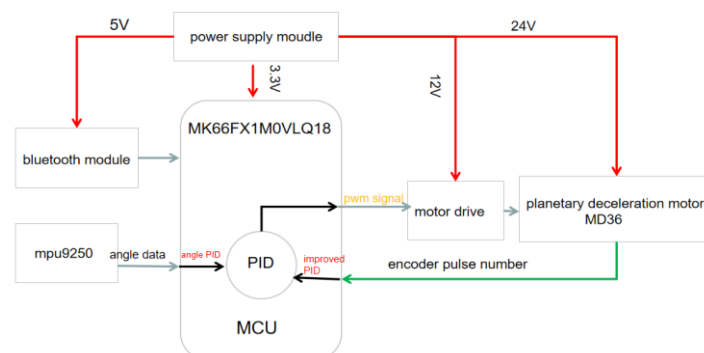


**Figure 2.** Schematic diagram of the circuit of the experimental device

Considering the price/performance ratio, the mobile system's MCU main control module uses the MK66FX1M0VLQ18 (K66) based on the minimum system, which can perform various data calculations and quickly process feedback information. The power supply module, divided into 3.3v, 5V, 12V and 24V circuits, acts on different circuit modules. Angle acquisition module adopts MPU9250, which integrates high-precision gyroscopes, accelerometer, and geomagnetic sensors. It can accurately measure the deviation angle between the actual direction and the preset direction of the mobile platform. The K66 generates pulse width modulation (PWM) [8] signal and drives planetary speed reduction motor through IR2104 motor driver. At the same time, K66 receives the motor speed information returned by the photoelectric encoder, which is processed by the algorithm to control the motor speed. The auxiliary debugging module is composed of Bluetooth module HC-05, which sends the speed of each Mecanum wheel to the host computer and the robot yaw error of the whole mobile platform.

## 3. The omnidirectional motion mechanism of the Mecanum wheel

In this paper, a set of four Mecanum wheels with a diameter of 152mm is used for the mobile platform. The many rollers are evenly distributed on the Mecanum wheel. The axis of the roller is at an angle to the wheel rim. Figure 3 shows the Mecanum wheel selected in this paper. The axle of the wheel and the rim are at an angle of  $45^\circ$ . The envelope of these rollers under the rotation of the wheel, coincide with the original circumferential surfaces of the wheel, which ensures that the wheels are attached to the

ground [9]. While the wheel is moving, the rollers on the wheel also rotate, which causes the frictional force in the circumferential direction of the roller to become the rolling friction force, which is negligible for the overall movement of the wheel. Therefore, the study of the movement of the wheel is only necessary to consider the force in the direction of the roller axis. Figure 4 shows the layout and kinematics of the Mecanum wheel used in this article. In this paper, the inverse kinematics model is used to calculate the speed of the four wheels according to the motion state of the chassis, so that the wheels can be controlled by the motor to make the car move at the specified speed and direction.

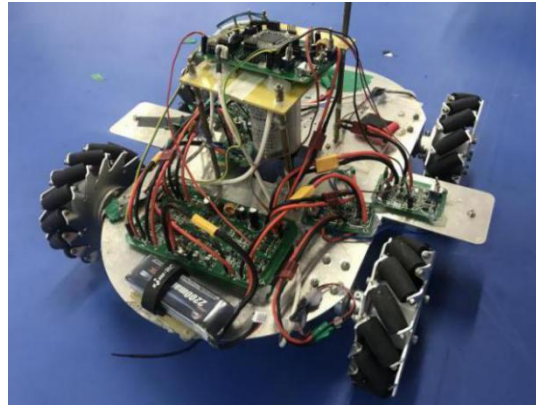


**Figure 3.** Physical map of the OMR

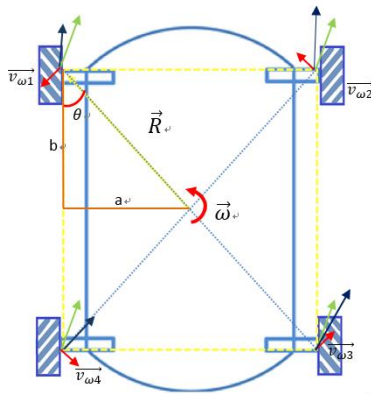


**Figure 4.** shows the layout and kinematics of the Mecanum wheel used in this article.

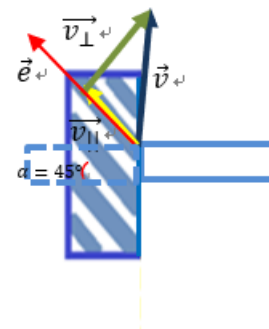


**Figure 5.** shows the speed breakdown of the rollers on the wheel.

The motion of the mobile platform is decomposed into X-axis translation, Y-axis translation, and yaw axis rotation. Then the movement of the car can be broken down into three vectors,  $\vec{v}_x$  represents the speed of the X-axis motion,  $\vec{v}_y$  represents the speed of the Y-axis motion,  $\vec{\omega}$  is the angular velocity of the yaw axis;  $\vec{R}$  represents the vector from the geometric center to the axis of the wheel, and  $\vec{v}$  represents the moving speed of the car. And the speed of the X-axis motion, the speed of the Y-axis motion, the moving speed of the car are,

$$\vec{v} = \vec{v}_t + \vec{v}_n \tag{1}$$

$$\vec{v}_x = \vec{v}_{tx} + \vec{\omega} \cdot \vec{R}_x \tag{2}$$

$$\vec{v}_y = \vec{v}_{ty} + \vec{\omega} \cdot \vec{R}_y \tag{3}$$

Analyze the speed of each wheel's axis position, taking wheel 1 as an example, the speed of the X-axis motion and the speed of the Y-axis motion are,

$$\vec{v}_{x1} = \vec{v}_{tx} - \vec{\omega} \cdot R \cdot \cos\theta = \vec{v}_{tx} - \vec{\omega} \cdot a \quad (4)$$

$$\vec{v}_{y1} = \vec{v}_{ty} - \vec{\omega} \cdot R \cdot \sin\theta = \vec{v}_{ty} - \vec{\omega} \cdot b \quad (5)$$

Analyze the speed of the rollers on the wheel: figure 5 shows the speed breakdown of the rollers on the wheel. Depending on the speed  $\vec{v}$  of the wheel axis position, the speed of the roller can be decomposed into a velocity  $\vec{v}_{\parallel}$  parallel to the roller axis and a velocity  $\vec{v}_{\perp}$  perpendicular to the roller axis, wherein the velocity perpendicular to the roller axis is the speed at which the roller rotates axially, so the wheel speed calculation ignores  $\vec{v}_{\perp}$ .  $\vec{e}$  is the unit vector along the direction of the roller.

$$\vec{v}_{\parallel} = \vec{v} \cdot \vec{e} = (\vec{v}_x + \vec{v}_y) \cdot (\vec{e}_x + \vec{e}_y) = -\frac{1}{\sqrt{2}} \vec{v}_x + \frac{1}{\sqrt{2}} \vec{v}_y \quad (6)$$

The speed of the wheel can be determined from the speed of the roller,

$$\vec{v}_{\omega} = \frac{\vec{v}_{\parallel}}{\cos\alpha} = \frac{\vec{v}_{\parallel}}{\cos 45^\circ} = \sqrt{2} * \left( -\frac{1}{\sqrt{2}} \vec{v}_{x1} + \frac{1}{\sqrt{2}} \vec{v}_{y1} \right) = -\vec{v}_{x1} + \vec{v}_{y1} \quad (7)$$

According to (4) and (5) and (7),

$$\vec{v}_{\omega 1} = -\vec{v}_{tx} + \vec{\omega} \cdot a + \vec{v}_{ty} - \vec{\omega} \cdot b \quad (8)$$

In the same way, the kinematic analysis of the remaining wheels can be performed, resulting in:

$$\begin{bmatrix} \vec{v}_{\omega 1} \\ \vec{v}_{\omega 2} \\ \vec{v}_{\omega 3} \\ \vec{v}_{\omega 4} \end{bmatrix} = \begin{bmatrix} -1 & 1 & a-b \\ 1 & 1 & -(a-b) \\ -1 & 1 & -(a-b) \\ 1 & 1 & a-b \end{bmatrix} \begin{bmatrix} \vec{v}_{tx} \\ \vec{v}_{ty} \\ \vec{\omega} \end{bmatrix} = \mathbf{J} \begin{bmatrix} \vec{v}_{tx} \\ \vec{v}_{ty} \\ \vec{\omega} \end{bmatrix} \quad (9)$$

J in (9) is the Jacobian matrix of the system inverse kinematics. Reference the matrix J in (5), it is known that  $\text{rank}(\mathbf{J}) = 3$ . Therefore, it can be guaranteed that the equation solution has one and only one solution. And the equation (8) reflects that as long as the angular velocities of the four wheels are controlled reasonably, various forms of motion can be realized.

#### 4. Improved PID algorithm from three aspects

With the advancement of technology and the maturity of engineering technology, the requirements for control accuracy are getting higher and higher, and the defects of classical PID control become more and more obvious. Along with these are various improved and innovative PID control methods, such as ADRC auto-disturbance PID, fuzzy PID and single neuron PID control methods.

The PID is divided into a continuous type PID and an incremental type PID. Continuous PID control is the analog PID control of analog signals. The formula is:

$$u(t) = K_p e(t) + K_i \int e(t) dt + K_d [e(t)] \quad (10)$$

$K_p$  is the proportional coefficient,  $K_i$  is the integral coefficient, and  $K_d$  is the differential coefficient?

The digital PID control, that is, the so-called discrete PID control, can be obtained after the continuous PID control is discretized by a certain discretization method:

$$u(t) = K_p [e(t) - e(t-1)] + K_i e(t) + K_d [e(t) - 2e(t-1) + e(t-2)] \quad (11)$$

Incremental PID only calculates the increment of the output, and avoids the original integral link taking up a large amount of calculated storage space, resulting in data overflow loss. In our omnidirectional mobile robot control system, sampling is performed at regular intervals, so we use incremental PID as the control core of the system [10].

In this paper, under limited hardware resource, for the omnidirectional mobile robot control system, the classic incremental PID is improved in three aspects, namely the following integral separation, anti-integral saturation, and incomplete differential three major improvements.

#### 4.1. The Integral Separation PID Improvement

When the omnidirectional mobile robot is started or shifted to a specified value, the accumulation of points will occur in a short time, causing the system to overshoot and oscillate. The integral separation method [11] can solve this problem just right. The basic principle is that when the deviation is large, that is, the deviation between the actual value and the ideal set value is large, the integral action is cancelled to avoid overshoot; and when the deviation is small, add integral action to eliminate steady state error.

The improved PID control algorithm formula is:

$$u(t) = K_p[e(t) - e(t-1)] + \beta K_i e(t) + K_d[e(t) - 2e(t-1) + e(t-2)] \quad (12)$$

$\beta$  is called the integral switching coefficient, and its value range is:

$$\beta = \begin{cases} 1 & |e(t)| \leq e \\ 0 & |e(t)| > e \end{cases}$$

#### 4.2. Anti-Integral Saturation PID Improvement

In the mobile platform control system, it is possible that the system will accumulate deviations in a uniform direction, causing supersaturation; and to solve this problem, we introduce an anti-integration saturation method [12] to solve. The basic principle is: when calculating the current deviation  $e(t)$ , first judge the previous deviation  $e(t-1)$ . If the maximum limit of the omnidirectional mobile robot is exceeded, only the accumulation of negative deviation is performed.

The improved PID control algorithm formula is:

$$u(t) = K_p[e(t) - e(t-1)] + \alpha K_i e(t) + K_d[e(t) - 2e(t-1) + e(t-2)] \quad (13)$$

$$\alpha = \begin{cases} 1 & (e(t-1) > \max \text{ and } e(t) < 0) \text{ or } (e(t-1) < \min \text{ and } e(t) > 0) \\ 0 & \text{other} \end{cases}$$

$\alpha$  we call the suppression saturation coefficient.

#### 4.3. Incomplete Differential PID Improvement

When we introduce the differential coefficient  $K_d$  it is easy to cause high-frequency interference to the omnidirectional mobile robot system. At this time, we can introduce a first-order low-pass filter to filter out high-frequency interference, so-called incomplete differentiation[13].

The improved incomplete differential PID formula is:

$$u(t) = K_p[e(t) - e(t-1)] + K_i e(t) + \gamma U_d(t) + (1 - \gamma)U_d(t-1) \quad (14)$$

$$U_d(t) = K_d[e(t) - 2e(t-1) + e(t-2)] \quad (15)$$

$\gamma$  that we call the proportion of trust.

The basic structure diagram can be expressed as figure 6.

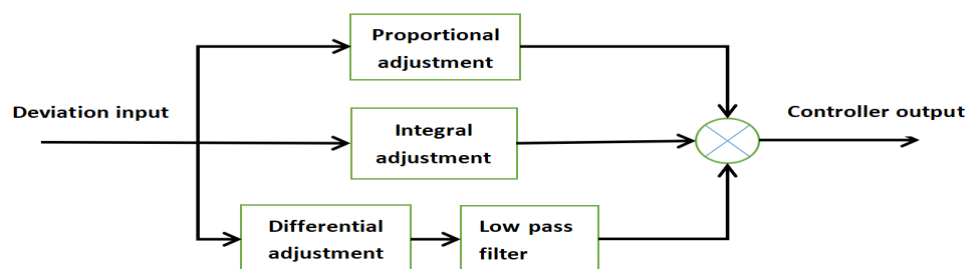


**Figure 6.** The basic structure diagram

#### 4.4. Combination and complementation of three improved methods

In order to improve the heading accuracy of mobile robots under limited hardware resource, this paper combines three improved methods to avoid overshoot of the system and quickly eliminate the steady-state error by integral separation. The anti-integration saturation prevents the deviation. Over-saturation caused by accumulation, but not completely differentiated, improves the anti-interference ability of the system and makes up for the shortcomings of the traditional PID control algorithm.

The overall control strategy of the improved system is shown in figure 7.

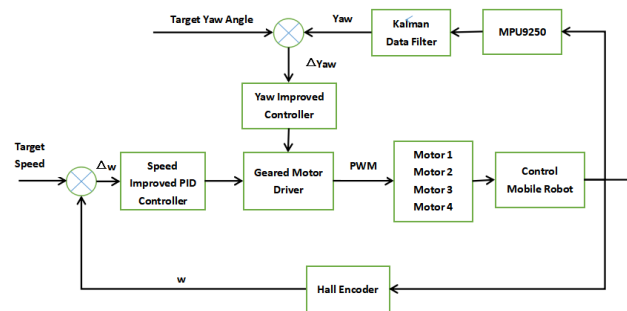


**Figure 7.** The overall control strategy

## 5. Actual Measurement Analysis

### 5.1 Analysis of experimental results with or without feedback angle adjustment

The OMR used in our experiments is shown in Figure 3. In the experiment, the robot's walking deviation is due to the uneven friction of the wheel and the internal mechanical structure of the four wheels. In the experiment, we divided the two cases to measure the lateral angle of the robot and the offset angle after 6 seconds of continuous motion. The first case is to use the feedback angle data of the MPU9250 to adjust the heading angle of the robot. The second case is the feedback angle data of the MPU9250 is not used to adjust the heading angle of the robot. The experiment analyzed the longitudinal and lateral movements of the robot for 6 seconds. We assume that the heading direction set for the robot is  $0^\circ$ , then the deviation angle (Yaw) between the actual heading of the robot and the set heading direction is shown in Figure 8. From the experimental data, after 6 seconds of motion, the longitudinal motion deviation angle of the robot does not exceed  $3^\circ$ , and the lateral motion deviation angle is as high as  $25.5^\circ$ . It is obvious that the lateral movement produces a larger heading angle deviation than the longitudinal movement. This is because when the robot moves laterally, it is necessary to use the friction generated by the rollers on the Mecanum wheel to counteract the force on the longitudinal component, thus causing a loss of speed during the friction transmission, which cannot be avoided.

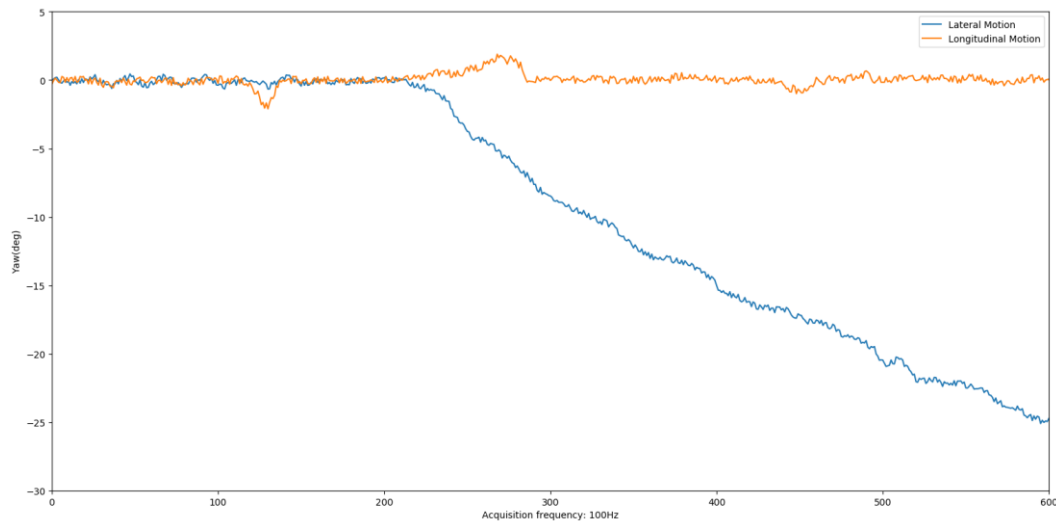


**Figure 8.** Robot's yaw without angle feedback

To solve the problem of heading offset of the robot, this paper proposes an improved PID algorithm, which uses the angle feedback information collected by the MPU9250 to correct the heading direction of the robot. Figure 9 shows the robot's heading angle changes during lateral and longitudinal directions when using the improved PID control algorithm. From the experimental results, we can easily find that the improved PID algorithm has a significant effect on adjusting the lateral motion state of the robot. And the results show that the robot's heading angle changes from  $-1.0$  to  $1^\circ$  during longitudinal motion, and from  $-1$  to  $0.5^\circ$  during the lateral motion.

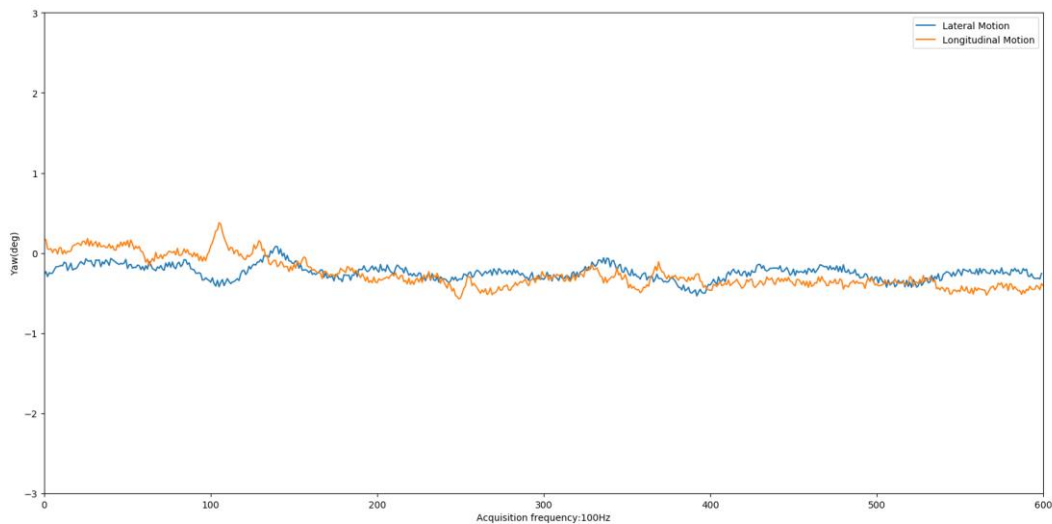


**Figure 9.** Robots yaw in the improved PID control

### 5.2 Analysis of Experimental Results of Improved PID Algorithm for System Response Speed

We used Bluetooth as a debugging aid to measure the number of pulses returned by the encoder of the motor corresponding to the four wheels as measurement data, return to the computer via Bluetooth, and export the effect of drawing the graph analysis test.

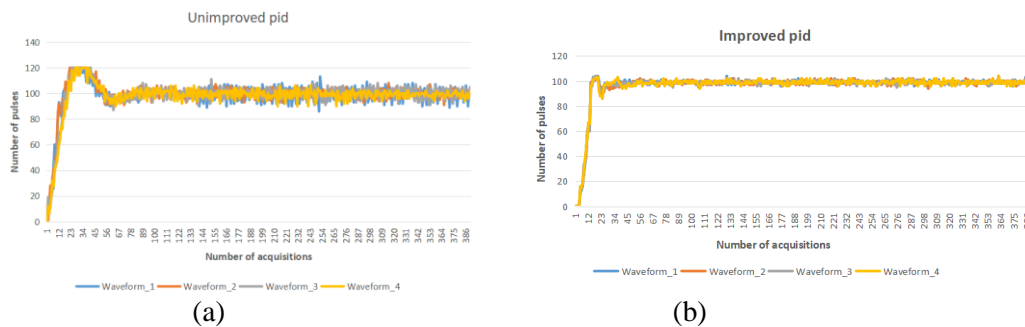


**Figure 10.** Traditional PID and improved PID actual measurement curve

In figure 10(a), it shows the actual measurement curve of the traditional PID before improvement. The frequency of the pulse acquisition data is 50Hz, so we can easily see from the figure 10(a) that the response speed of the traditional PID is about 1.78-2.0s. Not only that, the traditional PID algorithm obviously shows the speed overshoot phenomenon. Figure 10(b) is the actual measurement curve of the improved traditional PID. The response speed of the improved PID is nearly 1.2-1.3s, which represents a 20-30% improvement in response speed compared to traditional PID algorithms. In figure 10(b), we can see from the graph that the first-order low-pass filter designed by the algorithm filters out the high-frequency interference. At the beginning, when the deviation is large, there is little overshoot, and when the deviation is smaller than our setting. Adding the integral term to the threshold eliminates the steady-state error. It can be seen that the curve after the improvement is relatively flat, and the four waveforms are basically coincident, indicating that the speeds of the four wheels tend to be consistent. After several sets of experimental tests, we can obtain the multiple sets of comparative data shown in Table 1.

**Table 1.** Improved pulse data statistics of PID algorithm

Ideal number of pulses	Response time(s)	Overshoot amplitude rate	Fluctuation range
100	1.2-1.3	-10.8%-5.4%	5-10 pulses
120	1.6-1.7	-12.6%-6.2%	7-11 pulses
140	2.3-2.5	-13.2%-6.5%	8-15 pulses

## 6. Conclusion

In this paper, in order to improve the OMR course accuracy under limited hardware resource, an improved PID algorithm is proposed.

Through the improvement of the traditional PID in three aspects: the integral separation method, the anti-integral saturation method and the incomplete differential method, the response time of the system is improved. By using the improved PID algorithm and the angle data returned by MPU9250, It skillfully solves the problem of deviation caused by the skidding of the fetal membrane in the process of motion of the mobile robot, avoids the overshoot phenomenon at the beginning of the operation of the mobile robot, and filters out the high frequency interference of the mobile robot. Experimental data shows that the lateral heading angle of the robot after 6 seconds of continuous lateral motion has dropped from  $-15.5^\circ$  at the beginning to  $-1-0.5^\circ$  and then the settling time of the improved PID control algorithm was improved by 0.58-0.7s and that the overshoot speed decreased about 10% in the motion. The stability and anti-jamming performance of mobile robot are improved. This improved algorithm is certainly not the best, but in the case of limited system hardware environment, we have been able to achieve good results. We will further improve the PID algorithm and the control strategy of the system in the future work, and strive to break through the limited hardware resource, so that it is well suited to different hardware environments.

## References

- [1] I. Carlos, "Stabilization of the PVTOL aircraft based on a sliding mode and a saturation function," *International Journal of Robust and Nonlinear Control*, vol. 27, no. 5, pp. 79-85, March 2016.
- [2] Y. Zhang and G. Z. Zhu, "Research on the omni-directional mobile platform technology based on the Mecanum wheel," *Modern Manufacturing Technology and Equipment*, vol. 128, no. 2, pp. 14-16, March 2017.
- [3] Z.Q.Yu,X.H.Yin, Z. Cao,B.B.Yao, G.Liu,and H. Zhao,"Design of the control system for laser guiding AGV,"*Advanced Materials Research*,vol.650,no.54, pp. 488-492, September 2013.
- [4] T. Jilek, F. Burian, V. Kriz, *Kinematic Models for Odometry of a Six-Wheeled Mobile Robot*,IFAC-PapersOnLine, Volume 49, Issue 25, 2016, Pages 305-310,
- [5] Pouya Panahandeh, Khalil Alipour, Bahram Tarvirdizadeh, Alireza Hadi, A kinematic Lyapunov-based controller to posture stabilization of wheeled mobile robots, *Mechanical Systems and Signal Processing*, Volume 134,2019,106319,ISSN 0888-3270,
- [6] Zheng-cai CAO, Ying-tao ZHAO, Yi-li FU, Research on point stabilization of a wheeled mobile robot using fuzzy control optimized by GA, *The Journal of China Universities of Posts and Telecommunications*, Volume 18, Issue 5, 2011, Pages 108-113, ISSN 1005-8885,
- [7] Huang H C , Wu T F , Yu C H , et al. Intelligent fuzzy motion control of three-wheeled omnidirectional mobile robots for trajectory tracking and stabilization[C]// *International Conference on Fuzzy Theory & Its Applications*. IEEE, 2013.
- [8] Holtz J. Pulsewidth modulation--A survey[J]. *IEEE Trans.ind.electro*, 1992, 39(5):11-18 vol.1.
- [9] Shi Yonglin, Design and implementation of autonomous navigation omnidirectional mobile platform in a structured environment [D]. Zhengzhou University. 2019
- [10] Xiao Wenjian, Li Yongke. Design of Intelligent Vehicle Based on Incremental PID Control Algorithm[J]. *Information Technology*, 2012(10): 125-127.
- [11] Guo Yijun [1], Li Haijun [2], Duan Xinglin [1]. Design of incremental integral separation PID controller based on S7-200[J]. *Industrial Instrument & Automation*, 2007(6).
- [12] Wang Haochen. Research on Motor Control Based on Anti-Integral Saturated Incremental PID Algorithm[J].*Electric Drive Automation*,2017,39(06):10-13.
- [13] Chen Ping. Application Research of Incomplete Differential PID Control[J]. *Electromechanical Technology*, 2006, 29(4): 31-32.